Nano Energy 63 (2019) 103861

Contents lists available at ScienceDirect

Nano Energy

journal homepage: www.elsevier.com/locate/nanoen

Full paper

Mechanoluminescence enhancement of ZnS:Cu,Mn with piezotronic effect induced trap-depth reduction originated from PVDF ferroelectric film

Fulei Wang[a], Fuling Wang[b], Xiandi Wang[c], Shicai Wang[a], Jianfeng Jiang[d], Qilu Liu[a], Xiaotao Hao[a,b], Lin Han[d], Jianjun Wang[a], Caofeng Pan[c,**], Hong Liu[a,e,*], Yuanhua Sang[a,***]

[a] State Key Laboratory of Crystal Materials, Shandong University, Jinan, 250100, China
[b] School of Physics, Shandong University, Jinan, 250100, China
[c] Beijing Institute of Nanoenergy and Nanosystems, Chinese Academy of Sciences, Beijing, 100083, China
[d] Institute of Marine Science and Technology, Shandong University, Qingdao, 266000, China
[e] Institute for Advanced Interdisciplinary Research (iAIR), University of Jinan, Jinan, 250022, China

ARTICLE INFO

Keywords:
ZnS:Cu,Mn
Mechanoluminescence
Piezoelectric effect
Trap-depth

ABSTRACT

Mechanoluminescence is a light emission process that is induced by a mechanical stimulus. The mechanisms that have been proposed to mediate this effect include elastic potential energy conversion and piezoelectric field-induced release of trapped charges for recombination. However, how to enhance this phenomenon is an open question for the application of mechanoluminescent (ML) effect. Herein, an effective ML enhancement approach was suggested through piezotronic effect driven trap-depth reduction of typical ML material (ZnS:Cu,Mn) based on charge release of ferroelectric polyvinylidene fluoride (PVDF) film. The experimental results illustrated that a layer of PVDF film covered on the both sides of ZnS:Cu,Mn ML layer can be nearly double the ML intensity in the particular external pressure, compared to that of the individual ZnS:Cu,Mn films. The films with an enhanced ML property show high potential for use in real-time pressure mapping systems, smart sensor networks, high-level security systems, and artificial intelligence.

1. Introduction

Mechanoluminescence is a nonthermal luminescence induced by mechanical stress applied to solids and was first discovered in 1605 [1]. However, due to the weak and unrepeatable properties of mechanoluminescent (ML) materials prohibit the practical applications of materials/device in some important cases. With the introduction of new ML materials, especially $SrAl_2O_4$:Eu,Dy [2] and doped ZnS [3], intense and reliable mechanoluminescence has been found; these materials possesses the potential for application in tactile imaging, light sources, and fracture or stress sensors and have applications in information security [4–6], among other fields.

As is well known, the emission of light is the originated from the transition of electrons from the excited state to the ground state of active ions. Typically, a large number of charge carriers form at the beginning of the synthesis of a material or under the illumination of light. The charge carriers are trapped at various defects, such as donors and acceptors. In the process of ML, the mechanical stimuli induce the charges released to the conduction and valance band. The recombination of the charges would occur and releases the stored energy by non-radiation to the doping ions. Then the excited doping ions emit photons to release the energy. The detrapping of carriers in phosphors under proper mechanical stimuli is the essential step for the ML process. There are three main mechanisms to initiate the detrapping of charge carriers, such as the movement of a dislocation during elastic and plastic deformation [7], the internal electric field generated from domain structures [8], and the internal electric field based on the piezoelectric property [9,10]. Among these processes for the release of trapped carriers, the process based on the piezoelectric property has attracted extensive interest [11–14].

The doped ZnS phosphor possesses great advantages as an ML phosphor. Copper or manganese doping of a ZnS matrix creates a ZnS-based ML phosphor free of the preirradiation for repetitive luminescence [15]. ZnS:Cu has realized repetitive luminescence under mechanical stress over a hundred-thousand times without requiring additional treatment [16]. This property eliminates the limitation of ML

* Corresponding author. State Key Laboratory of Crystal Materials, Shandong University, Jinan, 250100, China.
** Corresponding author.
*** Corresponding author.
E-mail addresses: cfpan@binn.cas.cn (C. Pan), hongliu@sdu.edu.cn (H. Liu), sangyh@sdu.edu.cn (Y. Sang).

https://doi.org/10.1016/j.nanoen.2019.103861
Received 25 May 2019; Received in revised form 17 June 2019; Accepted 27 June 2019
Available online 28 June 2019
2211-2855/ © 2019 Elsevier Ltd. All rights reserved.

phosphors in practical applications. Although the mechanism behind the self-recovery of ZnS-based ML phosphors is still unclear, the enthusiasm to study potential applications has not been reduced. ZnS:Mn microparticles have been used to construct sensors for various applications [17–21]. To realize an efficient mechanoluminescence-based sensor, the mechanical stimulation and the enhancement of the ML property are the most attractive points. Various of devices have been proposed to realize ML energy conversion via various signals [17,18,22,23]. For instance, devices could be stimulated by an ultrasound signal and could show a visual response by the integration of a PMN–PT substrate with a converse piezoelectric effect [23]. However, the light emission of ZnS:Mn was claimed to be an electroluminescent (EL) process driven by the piezoelectric potential, which was generated from the converse piezoelectric effect of a PMN–PT substrate. Later, upon integration with a magnetic Fe–Co–Ni-PDMS composite laminate, the magnetic variation induced a relative mechanical stress by the magnetic laminate, which then realized a visible-light emission based on a ZnS:Mn,Al,Cu phosphor [22]; this action allowed the device to be operated by a magnet. There have also been designs beside material synthesis to enhance the ML property [18,24,25]. A flexible matrix was introduced to improve the pressure loaded on the ZnS:Mn phosphor. Therefore, a better sensitivity to pressure and a higher resolution were achieved with this full dynamic-range pressure sensor matrix. Even personalized handwriting could be distinguished [18]. The principle behind the improved ML response remains the increase in the pressure loaded on the ML phosphor, and it is the most acceptable strategy to design mechanoluminescence-based devices [15–17, 20.

As is well known, the electric field plays an important role in the release of trapped carriers. Many kinds of ML phosphors have also been implemented in EL devices [26–28]. Therefore, the reduced trap-depth can be realized by the application of an electric field. Moreover, the ML process from the doped ZnS phosphor is too complicated to be discussed according to the internal electric field induced by the piezoelectric property. There are many shallow traps in the ZnS matrix that should be easily stimulated by mechanical stress [29]. However, the EL process requires a high electric field, which is approximately 100 times larger than the estimated electric field induced by the piezoelectric property of ZnS [26]. This notion indicates that there should be some deeply trapped carriers that cannot be motivated by the internal electric field. A high dynamic load with a high strain rate or an electric field application would release the carriers in deeper traps [30]. The generation of an electric field without an external power source would benefit the practical applications of the device. Piezoelectric materials can generate electricity from pressure and require the same conditions as the ML phosphor. Therefore, it should be easy to integrate an external electric field acting on the ML phosphor to enhance the ML emission.

Therefore, in the current work, the design of a multilayered ML device is proposed by integrating a Mn and Cu coactivated ZnS phosphor and polyvinylidene fluoride (PVDF). In the device, the ZnS:Cu,Mn phosphor is the ML response layer. The PVDF layer, which covers the ML layer, is designed to provide the external electric field to enhance the ML response of the ZnS:Cu,Mn phosphor. The ML response in this device is improved. Combined with the evaluation of the piezoelectric property by Piezoelectric Force Microscope (PFM), the mechanism of the enhancement of the ML property based on the external piezoelectric field is discussed. This self-powered design with enhanced ML response could benefit the device in practical applications.

2. Experimental procedures

2.1. Materials and devices

The sandwich ML device was constructed by integrating supporting layers, ML active layer and PVDF layers, and was packaged by polyethylene terephthalate (PET) layers. Briefly, ZnS:Cu,Mn microparticles (50–250 mg, purchased from Obest, China) were ultrasonically dispersed in 10 ml ethanol to form a slurry with various concentration. A transparent cylinder mold was placed at the center of a thermoplastic ethylene-vinyl acetate copolymer (EVA) thin film (40 mm × 40 mm, this layer and the PET layer were peeled from thermoplastic papers purchased from Deli, China). The slurry was rapidly poured into the transparent cylinder mold. After drying at room temperature, the ZnS:Cu,Mn microparticles formed a relatively uniform film. The phosphor film on EVA was packaged with PET in a thermal molding machine. PVDF piezoelectric thin films (56 μm in thickness, Fig. S1 in the supporting information; MEAS, USA) individually or packed with the ZnS:Cu,Mn phosphor films were evaluated to study their effect on ML enhancement. An interdigital electrode type of electroluminescence (EL) device with the ZnS:Cu,Mn phosphor was also prepared to compare with the ML device. The fabrication and properties of the EL device are shown in the supporting information (Fig. S2).

2.2. Characterization

The crystallization structures of the ZnS:Cu,Mn phosphor and PVDF were characterized by X-ray powder diffraction (XRD) using an X-ray diffractometer (Bruker D8 Advance, Germany, Cu Kα). The morphology of the samples and the composition quantitative analysis were studied by an electron probe microanalyzer (EPMA-1720H, Shimadzu Corporation, Japan). The thickness of the luminescent layers was characterized with a digital microscope (VHX-1000, Keyence, Japan). The piezoelectric potential of the PVDF film was carried out using an oscilloscope (DSO-X3014A, Agilent, USA). The conductive Ag colloid electrodes were used to connect to the oscilloscope poles. The PFM (Bruker Dimension Icon Scanning Probe Microscope with a SCM-PIT, Pt-coated conductive tip, with the contact mode, Germany) was used to characterize the piezoelectric properties of ZnS and PVDF. Before the measurement, the powders were well dispersed in alcohol and then dropped on an Au-coated silicon wafer, for which the thickness of the Au film was ~50 nm. After annealing at 120 °C for 24 h, another ~5 nm Au layer was coated via magnetron sputtering to achieve the proper conductivity. The field-effect transistor (FET) is a transistor that uses an electric field to control the electrical behavior of the device. In this device, the gate-to-source voltage determines the level of constant current through the drain-to-source channel [31,32]. Thus, the common use of a FET device is as an amplifier, which evaluates V_{gs} (the voltage between the gate and source) by testing I_{ds} (the current through the drain to the source). The piezoelectric potential of the PVDF film load was measured by the FET as V_{gs} (Note S1 in the supporting information). The piezoelectric field of the PVDF was simulated by COMSOL with the MEMS module [33]. The spatial distribution of the electric field induced by the piezoelectric response of PVDF was also simulated. The FTIR spectrum of PVDF film was recorded by a Fourier-transform infrared spectrometer (FT-IR, Nexus 670, Thermo, USA). The transmittance of devices with various thicknesses of the ZnS:Cu,Mn phosphor layer were measured by a direct light detector (UH4150 spectrophotometer, Hitachi, Japan).

A manual set was integrated to test the ML spectrum at a fixed pressure during its scan of the ZnS:Cu,Mn-based ML devices. Basically, with a proper loading, the contact point of a force gauge (HandpiHP-50) was fixed and coupled with the optical fiber of a spectrometer (NOVA highly sensitive spectrometer, Ideaoptics, China). During the scan of the ML devices at a fixed speed, the luminescent intensities were collected by the spectrometer in the range of 300–1100 nm.

3. Results and discussion

The morphology and composition of the ZnS:Cu,Mn phosphor and PVDF film are shown in Fig. 1. The SEM image shows that the size of the particles are homogeneous of ~23 μm (Fig. 1a). There are only a few small particles; however, these particles would benefit the ML emission due to the smaller contact areas between particles, which leads to a

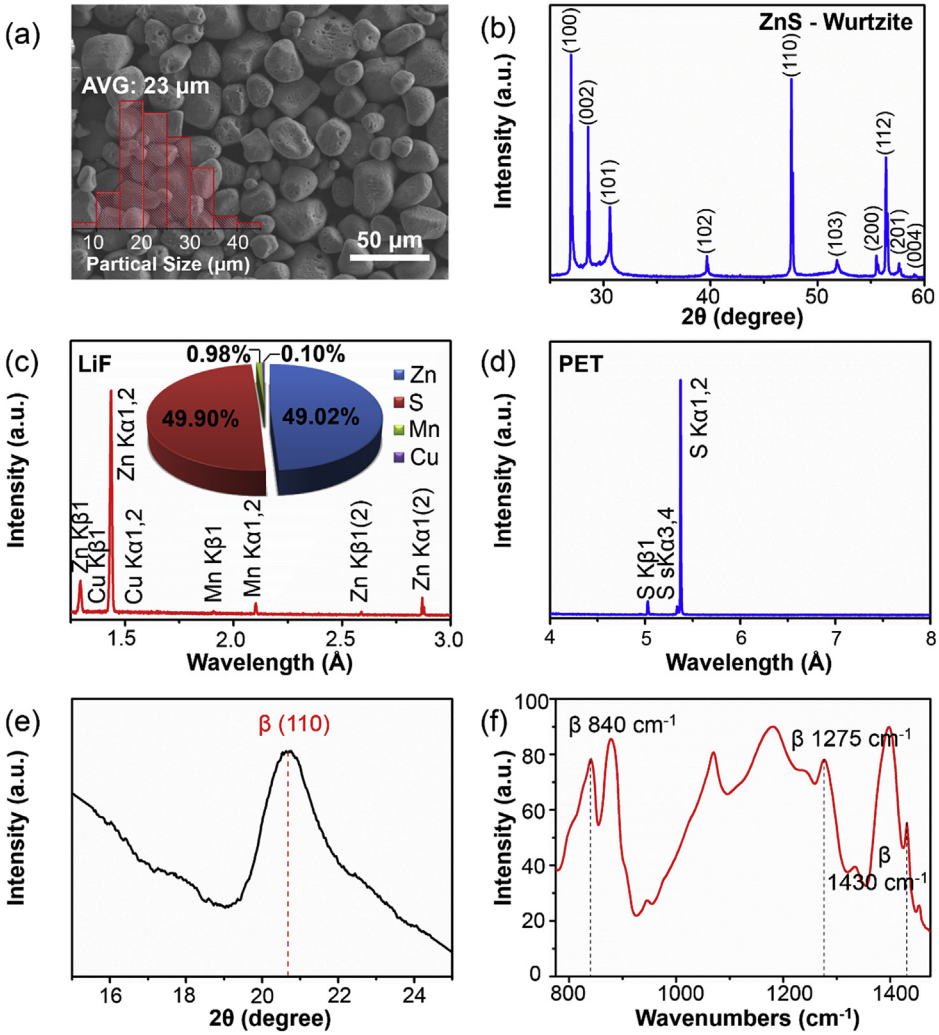

Fig. 1. (a) SEM image of the phosphor particles of ZnS:Cu,Mn. The inset shows the statistical results for the ZnS:Cu,Mn particle size, with an average value of 23 μm. (b) The XRD pattern of the phosphor. (c) and (d) The EPMA qualitative elemental analysis of the phosphor using the waveband of LiF and PET crystals, respectively. The inset is the component breakdown determined by the EPMA quantitative elemental analysis. (e) The XRD pattern of the PVDF film. (f) The FTIR spectrum of the PVDF.

higher-pressure loading on the particles. All the diffraction peaks in the XRD pattern can be assigned to the ZnS wurtzite structure (PDF card No. 36–1450) (Fig. 1b). This result confirms the pure phase of ZnS and the perfect crystallinity. Fig. 1c and d shows the qualitative results of the phosphor obtained by EPMA. There are only the peaks corresponding to Zn, Mn and Cu observed in the wavebands of the LiF analyzing crystal, while the peaks corresponding to S are detected in the wavebands of the PET analyzing crystal. The doping concentrations of Mn and Cu in ZnS are 0.98% and 0.10%, respectively, which are consistent with the proposed concentrations. The concentration analysis reveals that the doping ions are positioned at the Zn lattice site (Inset of Fig. 1c). As is well known, only β-phase PVDF has been proposed to have the best piezoelectric property. The XRD pattern of the poled PVDF film only shows the (110) peak at 20.6°, demonstrating the β phase of PVDF (Fig. 1e). The peaks of FTIR spectrum can be assigned as the characteristic absorption bands of PVDF at 840 cm^{-1} (CH_2 rocking), 1275 cm^{-1} (trans band), and 1430 cm^{-1} (CH_2 bending) [34,35], which further confirm the single β phase of PVDF.

The design of the layer-by-layer structure of the ML device is illustrated in Fig. 2a. Basically, proceeding from the inner to outer layer, the layers are ZnS:Cu,Mn phosphor, PVDF film, EVA film, and PET film, which form a triple sandwich structure. By changing the PVDF layer, e.g., with PVDF, without PVDF, and with one side PVDF, various ML devices were fabricated. In the devices, the wurtzite ZnS:Cu,Mn microparticles work as the ML response phosphor. The PVDF thin film was chosen to generate the external piezoelectric field under pressure, which was expected to enhance the ML property. The EVA layers were used to package the PVDF film and the ZnS:Cu,Mn layer due to its thermoplastic property. The PET films, based on their high toughness, were also used to protect the devices. All the organic films are almost transparent; they do not obstruct the luminescence from the ZnS:Cu,Mn phosphor.

To evaluate the luminescent intensity of the various devices, a manually generated set of measuring system was integrated, as shown in Fig. 4b. In this set, the contact point of the force gauge (HandpiHP-50) was fixed and coupled with an optical fiber to the spectrometer (500 μm in diameter). With a specific loading, the luminescent intensities were collected by the spectrometer in the range of 300–1100 nm during the horizontal glide of the ML devices. It should be noted that the coupling between the luminescent point and spectrometer contributed to the stability of the measured luminescent intensity. The luminescent spectrum of the ML device was recorded by the manual set and the operation. The luminescence is orange light between 524 and 710 nm with a center peak at ~593 nm (Fig. 2c), which corresponds to Commission Internationale de l'Éclairage (CIE) coordinates of (0.57, 0.40) (inset of Fig. 2c). Compared with the

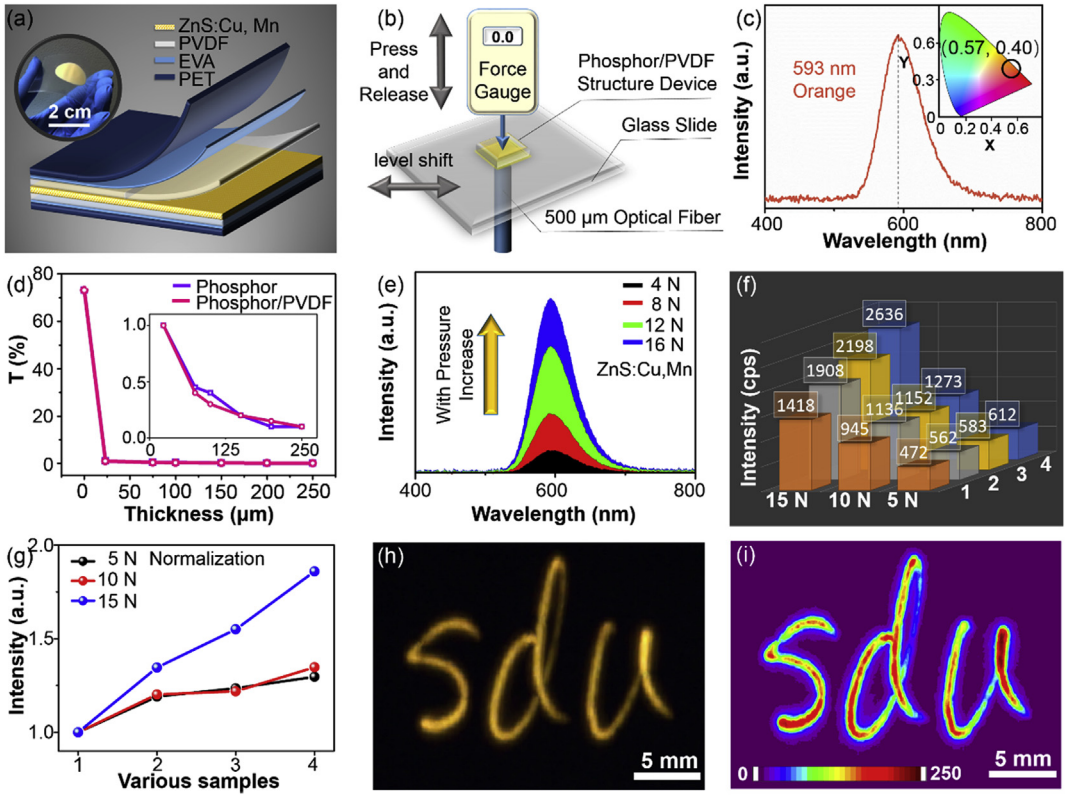

Fig. 2. (a) Schematic of ML device constructed as a layer-by-layer material. The inset is a photograph of the device. (b) A manual measuring system built to collect the mechanoluminescence. (c) The spectrum of the mechanoluminescence and its corresponding CIE coordinates. (d) The transmittance of the devices with various thicknesses of the ZnS:Cu,Mn layer. The inset is a zoom-in of the results for thicknesses from 30 μm to 250 μm. (e) The luminescent intensities of pure ZnS:Cu,Mn with increasing pressure. (f) The trends of the ML response under various loads with different structures at a wavelength of 593 nm. Structures 1–4 are the individual luminescence layer, luminescence layer with PVDF on the pressure side, luminescence layer with PVDF opposite the pressure side, and luminescence layer with PVDF on both sides, respectively. (g) The gradient of the luminescence intensity normalized to the results of the individual luminescence layer of the four structures under various pressures. (h) The dynamic luminescence trajectory generated from handwriting. (i) The extracted grayscale of the corresponding dynamic luminescence trajectory.

associated literature that previously discussed the luminescence peak of the ZnS:Cu,Mn phosphor at 588 nm, the ZnS:Cu,Mn we used exhibits a redshift due to either the Cu or Mn percentage or due to the size of the particles [36].

To understand the effect of the PVDF on the ML response, the ML emission should be compared. To quantitative characteristic the piezotronic enhancement response of the ML materials at a fixed quantity, we did the work as following. The transmittance of the devices with various thicknesses of the ML phosphor layer were measured at 593 nm (Fig. 2d). The one without the ML phosphor or PVDF film is 73.2%. With a film thickness of ~23 μm, the transmittance is only ~1%. With an increase in the thickness to 200 μm, the transmittance keeps decreasing to ~0.1%. In the current work, the thickness of the luminescent layer was controlled by the mass controls, as shown in Fig. S3 of the supporting information. According to the particle size of ZnS:Cu,Mn, shown in Fig. 1a, the luminescent layer of ~23 μm thick layer could be assigned as one layer of the ZnS:Cu,Mn particles, while the one with ~200 μm in thickness could consist of approximately with 8 layers of ZnS:Cu,Mn particles (Insets of Fig. S3 in the Supporting Information). This result indicates that only the ML emission from the first layer next to the light detector could be counted due to the heavy 593 nm light absorption of ZnS:Cu,Mn. Because the optical fiber detector is 500 μm in diameter, moreover, the ZnS:Cu,Mn particles are ~23 μm, there should be only ~200 ZnS:Cu,Mn particles contributing to the detected luminescence intensity. The variety of the luminescence intensity can reflect the ML response performance under various pressure, which should not be caused by the increase of the ML responded ZnS:Cu,Mn particles. All the samples with the PVDF film showed the same transmittance as that without PVDF. The application of the PVDF film will not influence the ML emission intensity.

The ML device without PVDF film was evaluated by the loading from 4 N to 16 N (Fig. 2e). With the increase in the loading, the ML intensity increases linearly. The ML intensities at the wavelength 593 nm with different structures under various pressures were recorded, as shown in Fig. 2f. The different structures marked as 1–4 are the individual luminescent layer, luminescent layer with PVDF at pressure side, luminescent layer with PVDF opposite the pressure side, and luminescent layer with PVDF at both sides, respectively. For the samples, the ZnS:Cu,Mn layer was ~100 μm to guarantee the number of the active ML particles. As shown in Fig. 2f, the ML response increases with both the increase of loading and the construction of PVDF film. The luminescence layer with PVDF on one side shows an enhanced ML response. Notably, the ML response of the one with PVDF at pressure side is a little weaker than that of the one with PVDF opposite the pressure side. Based on the good transparency of PVDF and no obvious absorption of the light at 593 nm (Fig. 2d), it is believed that the different detected ML responses were truly from the luminescence intensity. Considering with the poor transparency of the ZnS:Cu,Mn microparticles, the luminescence intensities detected were mostly from the surface particles next the spectrometer detector. Moreover, it can be expected that the piezoelectric field from the PVDF would reduce quickly with the increase of distance. The surface particles next to PVDF withstand a higher piezoelectric field produced by PVDF. Therefore, the ML response of the device with PVDF next to the detector is better than that of the pressure side. Moreover, with PVDF on both sides align in the same direction of polarization, the ML device shows the best ML

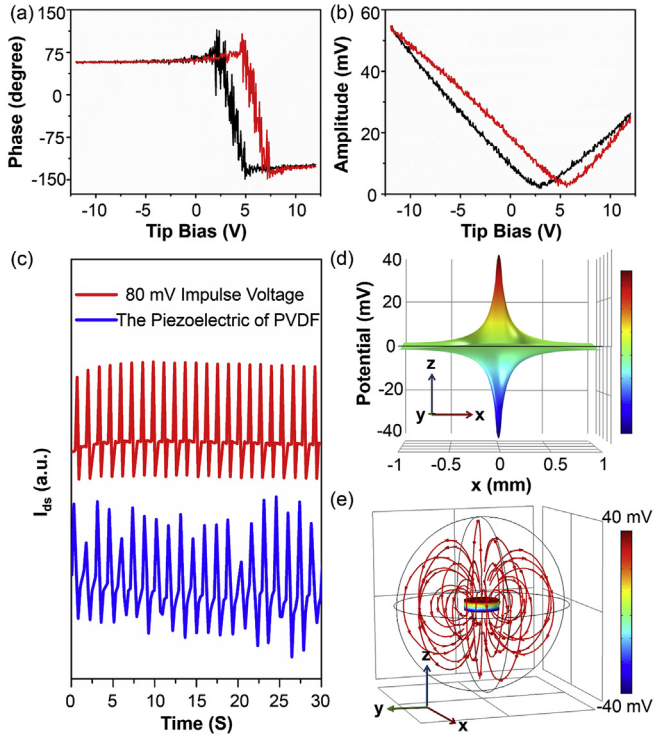

Fig. 3. The standard ferroelectric amplitude curve (a) and phase curve (b) of the ZnS:Cu, Mn at the ramp voltage from −12 V to 12 V. (c) The piezoelectric response of the PVDF film under pressure, as analyzed by FET. (d) The piezoelectric potential formation in 2D flat surface of PVDF film under 15 N, as simulated by COMSOL. A finite size of PVDF was used in the simulation for idealization. (e) The piezoelectric space field induced by the PVDF, as simulated by COMSOL.

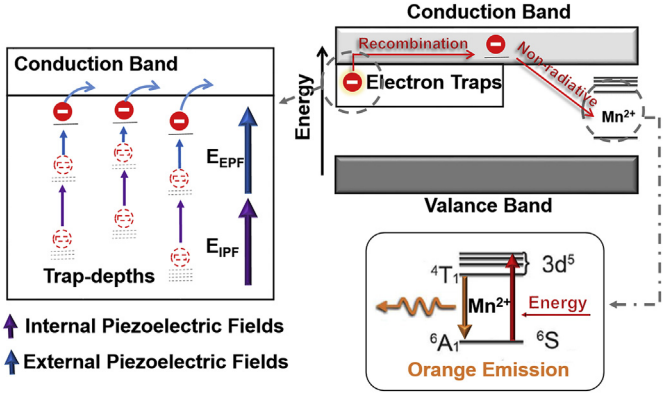

Fig. 4. The scheme of the ML enhancement of ZnS:Cu,Mn constructed with a PVDF film including the carrier trap and energy transfer.

response. This result indicates that a stronger external piezoelectric field induced by PVDF would result in a better ML response. To further discuss the improvement in the ML property of the structures, the normalized ML intensities were analyzed according to that of the individual luminescence layer at pressures of 5 N, 10 N, and 15 N (Fig. 2g). The improvements in the ML performance between device 1 and device 4under 5 N and 10 N of pressure are similar, reaching approximately 30% when PVDF is included on both sides; the improvement is quite significant under 15 N pressure (approximately 85%). This result indicates that the ML devices with PVDF can improve the ML property but prefer a high-pressure loading to achieve a significant improvement. This response might be due to the release of deep-trapped charges requiring a relatively strong external piezoelectric field. Further discussion about the different polarity of PVDF film resulting indifferent luminescence enhancement can be found in Fig. S4 in the Supporting Information.

The ML property of the device was recorded by the charge-coupled device (CCD) camera connected to a laptop as a light emission capture unit. With the image processing software programmed [24], this image acquisition system was used to acquire the handwritten characters of “sdu” (Fig. 2h). The pen without ink has a 1 mm tip in diameter. The full-image was integrated from a series of frames that were exhibited at an interval of 0.25 s. Moreover, the relative luminescent intensity could be assigned to the corresponding pressure (Fig. 2i). This result indicates that the handwriting habit can be distinguished by the different pressures applied during the writing.

To discuss the ML property of ZnS:Cu,Mn and the enhancement of the ML property with the construction of a PVDF film, the piezoelectric properties of ZnS and PVDF were studied via PFM and FET (Fig. 3a–c), and their piezoelectric fields were simulated via COMSOL (Fig. 3d and e). The piezoelectric hysteresis and butterfly loops are observed at voltages between −12 V and 12 V. The phase-tip bias and amplitude-tip bias loops match each other well. The rhomboid phase hysteresis loop and “butterfly shape” amplitude loop indicate the characteristic piezoresponse and distinct polarization switching behavior. Furthermore, the positive shift in the amplitude loop implies the existence of internal electric field in the wurtzite ZnS.

The piezoelectric potential of the PVDF film induced by a mechanical stress load was evaluated by the FET. As shown in Fig. 3c, the currents (I_{ds}) measured under a simulated V_{gs} of 80 mV and the V_{gs} from the piezoelectric response of PVDF are similar. Based on the control of I_{ds} by V_{gs}, the result indicates that the piezoelectric potential of PVDF with a load of 15 N is approximately 80 mV. Some other methods were also performed to confirm the piezoelectric potential of PVDF, such as the potential measurement by oscilloscope (Fig. S5), and PFM analysis (Fig. S6) in the Supporting Information. The piezoelectric potential of PVDF under a pressure of 15 N will reach the maxim of ± 40 mV at the center of pressure, and it will drop sharply with increase the distance outward the pressure applying center (Fig. 3d). This observation indicates that the piezoelectric potential shows the characteristic property of point-located charges, which would benefit the accuracy of the ML device without its extensive effect on the luminescence layer. Moreover, the piezoelectric space field induced by the PVDF shows a quick decay along the pressure direction (Fig. 3e). This result indicates that the effective range of the piezoelectric field is short. That effect is why the ML response of the device with PVDF at pressure side is a little weaker than that of the device with PVDF at the other side.

According to the piezoelectric properties of ZnS and PVDF discussed in Fig. 3, we propose a possible mechanism for the ML enhancement of ZnS:Cu,Mn integrated with PVDF films (Fig. 4). As is well known, the ZnS:Cu,Mn is also an EL phosphor [15,37]. The introduction of a PVDF film could induce an external piezoelectric field that might result in the EL response of mechanoluminescence, thus improving the luminescent intensity of ZnS:Cu,Mn. The EL response of the ZnS:Cu,Mn phosphor with respect to the DC voltage is weak (Fig. S7 in the supporting information). The luminescent intensity was less than 200 arbitrary units even at 6.0×10^5 V/m, which is very weak compared to the 1000-fold arbitrary units increase achieved with double-side PVDF (Fig. 2f). The pressure-induced piezoelectric field of the double-side PVDF is less than 1.6×10^3 V/m (Fig. 3c). Therefore, the impact ionization from the EL response induced by the piezoelectric field of PVDF should not be the reason for the ML enhancement. Nevertheless, the piezoelectric field induced by the PVDF cannot reaches the threshold of the charge carriers released, which required an external field on the order of 10^5 V/cm [38]. According to the ML mechanism of luminescence induced by an internal electric field, the piezoelectric field releases the trapped electrons to the valance band (VB) of ZnS [39]. The released charges recombine and release energy nonradiatively. The released energy transfers to the Mn^{2+} and excites it [40]. The de-excitation of Mn^{2+}

contributes to the orange emission, which is the characteristic emission of Mn^{2+} in the ZnS matrix. Although many works have been performed to clarify the mechanism of mechanoluminescence in a piezoelectric matrix, the key research direction has been to improve the electric field applied on the trapped charges [41]. The release of more trapped charges has been expected, therefore, realizing an enhanced ML response. Considering the clear enhancement in ML response by integrating PVDF and in the piezoelectric property of ZnS and PVDF, we propose the enhancement as follows. The deformation of ZnS:Cu,Mn induces an internal piezoelectric field that releases most of the trapped charges in shadow traps, while the PVDF-generated external piezoelectric field reduces the trap-depth, as shown in Fig. 4. Therefore, more trapped charges can be released to the bands, leading to the increase in energy that can excite more Mn^{2+} in ZnS. Finally, the de-excitation of the excited Mn^{2+} gives rise to the brighter emission.

4. Conclusion

In this work, a ZnS:Cu,Mn/PVDF multilayer sandwich structure was designed as an ML device to realize an enhanced ML response. The ML performance of the ZnS:Cu,Mn/PVDF ML device has achieved an ~85% improvement compared with the individual ZnS:Cu,Mn layer. The piezotronic effect of PVDF under pressure supplies an external piezoelectric field that can reduce the trap-depth of charges in ZnS matrix. More trapped charges, especially the deep-trapped charges would be released by the in-situ internal piezoelectric field of ZnS matrix, resulted in the improved ML property. This integrated structure converts the mechanical stress into ML process and external piezoelectric field simultaneously. This passive ML enhanced device was more facile to improve the mechanical stress detection. Therefore, it presents broad applications for real-time mechano-electric-photo transformation.

Acknowledgement

The authors wish to acknowledge funding of National Key Research and Development Program of China (2017YFE0102700), National Natural Science Foundation of China (Grant Nos. 51732007), Natural Science Fund for Distinguished Young Scholars of Shandong Province (ZR2019JQ16, JQ201814), and the Fundamental Research Funds of Shandong University (2018WLJH64). The authors are grateful to M. S. Zhu for assistance in experimental testing.

Appendix A. Supplementary data

Supplementary data to this article can be found online at https://doi.org/10.1016/j.nanoen.2019.103861.

References

[1] N.C. Eddingsaas, K.S. Suslick, Nature 444 (2006) 163.
[2] C.N. Xu, C. Li, Y. Imai, H. Yamada, Y. Adachi, K. Nishikubo, Adv. Sci. Technol. 45 (2006) 939–944.
[3] D.R. Reddy, B. Reddy, Appl. Phys. Lett. 81 (2002) 460–462.
[4] N. Terasaki, H. Yamada, C.-N. Xu, Catal. Today 201 (2013) 203–208.
[5] N. Terasaki, H.W. Zhang, H. Yamada, C.-N. Xu, Chem. Commun. 47 (2011) 8034–8036.
[6] C.N. Xu, T. Watanabe, M. Akiyama, X.G. Zheng, Appl. Phys. Lett. 74 (1999) 1236–1238.
[7] J.P. Hirth, J. Lothe, Theory of Dislocations, second ed., Wiley, New York, 1982.
[8] X. Wang, C.N. Xu, H. Yamada, K. Nishikubo, X.G. Zheng, Adv. Mater. 17 (2005) 1254–1258.
[9] C.F. Pan, L. Dong, G. Zhu, S.M. Niu, R.M. Yu, Q. Yang, Y. Liu, Z.L. Wang, Nat. Photon. 7 (2013) 752–758.
[10] R.M. Yu, L. Dong, C.F. Pan, S.M. Niu, H.F. Liu, W. Liu, S. Chua, D.Z. Chi, Z.L. Wang, Adv. Mater. 24 (2012) 3532–3537.
[11] Y. Hui, T.M. Lei, Y. Qin, R.S. Yang, Nano Energy 59 (2019) 84–90.
[12] A. Alarawi, V. Ramalingam, H.C. Fu, P. Varadhan, R.S. Yang, J.H. He, Optic Express 27 (2019) A352.
[13] K. Tao, W. Hu, B. Xue, D. Chovan, N. Brown, L.J.W. Shimon, O. Maraba, Y. Cao, S.A.M. Tofail, D. Thompson, J.B. Li, R.S. Yang, E. Gazit, Adv. Mater. 31 (2019) 1807481.
[14] H. Yuan, T.M. Lei, Y. Qin, J.H. He, R.S. Yang, J. Phys. D Appl. Phys. 52 (2019) 194002.
[15] S.M. Jeong, S. Song, S.K. Lee, N.Y. Ha, Adv. Mater. 25 (2013) 6194–6200.
[16] S.M. Jeong, S. Song, S.-K. Lee, B. Choi, Appl. Phys. Lett. 102 (2013) 051110.
[17] S.M. Jeong, S. Song, K.-I. Joo, J. Kim, S.-H. Hwang, J. Jeong, H. Kim, Energy Environ. Sci. 7 (2014) 3338–3346.
[18] X.D. Wang, H.L. Zhang, R.M. Yu, L.F. Dong, D.F. Peng, A.H. Zhang, Y. Zhang, H. Liu, C.F. Pan, Z.L. Wang, Adv. Mater. 27 (2015) 2324–2331.
[19] X.D. Wang, M.L. Que, M.X. Chen, X. Han, X.Y. Li, C.F. Pan, Z.L. Wang, Adv. Mater. 29 (2017) 1605817.
[20] X.Y. Wei, X.D. Wang, S.Y. Kuang, L. Su, H.Y. Li, Y. Wang, C.F. Pan, Z.L. Wang, G. Zhu, Adv. Mater. 28 (2016) 6656–6664.
[21] Y.L. Zhang, Y.S. Fang, L. Jia, Q.H. Zhou, Y.J. Xiao, K. Zhang, B.B. Luo, J. Zhou, B. Hu, ACS Appl. Mater. Interfaces 9 (2017) 37493–37500.
[22] M.C. Wong, L. Chen, M.K. Tsang, Y. Zhang, J.H. Hao, Adv. Mater. 27 (2015) 4488–4495.
[23] Y. Zhang, G.Y. Gao, H.L. Chan, J.Y. Dai, Y. Wang, J.H. Hao, Adv. Mater. 24 (2012) 1729–1735.
[24] X.D. Wang, R. Ling, Y.F. Zhang, M.L. Que, Y.Y. Peng, C.F. Pan, Nano Research 11 (2018) 1967–1976.
[25] N.M. Rao, D.R. Reddy, B. Reddy, C.N. Xu, Phys. Lett. 372 (2008) 4122–4126.
[26] A. Feng, P.F. Smet, Mater 11 (2018) 484.
[27] X.Y. Fu, S.H. Zheng, J.P. Shi, H.W. Zhang, J. Lumin. 192 (2017) 117–122.
[28] C. Wu, S.S. Zeng, Z.F. Wang, Fu Wang, H. Zhou, J.C. Zhang, Z.P. Ci, L.Y. Sun, Adv. Funct. Mater. 28 (2018) 1803168.
[29] G. Garlick, A. Wells, M. Wilkins, J. Chem. Phys. 17 (1949) 399–404.
[30] Y. Chen, Y. Zhang, D. Karnaushenko, L. Chen, J.H. Hao, F. Ding, O.G. Schmidt, Adv. Mater. 29 (2017) 1605165.
[31] N.R. Malik, Electronic Circuits: Analysis, Simulation, and Design, Prentice Hall, Englewood Cliffs, NJ, 1995.
[32] G.-m. Carlos, S.M. Cherem, MOSFET Modeling for Circuit Analysis and Design, World Scientific, 2007.
[33] L.L. Zhao, Y. Zhang, F.L. Wang, S.C. Hu, X.N. Wang, B.J. Ma, H. Liu, Z.L. Wang, Y.H. Sang, Nano Energy 39 (2017) 461–469.
[34] H. Yu, T. Huang, M.X. Lu, M.Y. Mao, Q.H. Zhang, H.Z. Wang, Nanotechnology 24 (2013) 405401.
[35] Y.L. Zhao, Q.L. Liao, G.J. Zhang, Z. Zhang, Q.J. Liang, X.Q. Liao, Y. Zhang, Nano Energy 11 (2015) 719–727.
[36] R. Maity, K. Chattopadhyay, Nanotechnology 15 (2004) 812.
[37] W.D. Wang, F.Q. Huang, Y.J. Xia, A.B. Wang, J. Lumin. 128 (2008) 610–614.
[38] B. Chandra, V. Chandra, P. Jha, Phys. B 463 (2015) 62–67.
[39] D.O. Olawale, T. Dickens, W.G. Sullivan, O.I. Okoli, J.O. Sobanjo, B. Wang, J. Lumin. 131 (2011) 1407–1418.
[40] V. Wood, J.E. Halpert, M.J. Panzer, M.G. Bawendi, V. Bulovic, Nano Lett. 9 (2009) 2367–2371.
[41] B. Chandra, C. Xu, H. Yamada, X. Zheng, J. Lumin. 130 (2010) 442–450.

Fulei Wang obtained his B.S. degree at Huaqiao University in China in 2015. Now, he studies as Ph.D candidate in Prof. Hong Liu's group in State Key Laboratory of Crystal Materials, Shandong University, China since 2015. His research interests are the appilcation of the piezoelectric materials, especially its mechanical energy to electrical energy conversion properties and machanoluminescence mechanism.

Fuling Wang is currently a postgraduate candidate under the supervision of Prof. Xiao-Tao Hao in School of physics, Shandong University. Her current research interests focus on the photophysics and nanomorphology of organic solar cells.

Dr. Xiandi Wang received his PhD degree in condensed matter physics from the University of Chinese Academy of Sciences in 2016. Now he is an associate professor at Beijing Institute of Nanoenergy and Nanosystems, CAS since 2018. His research interests mainly focus on the fields of piezo-photonic effect and triboelectric nanogenerator for fabricating novel flexible large-scale tactile sensor matrix and stretchable electronics.

Shicai Wang is a Ph.D candidate in State Key Laboratory of Crystal Materials, Shandong University. He received his B.S. degree in physics from Shandong University in 2016. His current research is mainly focused on the acoustic microfluidics and nanomaterials for cell detection.

Jianfeng Jiang is a master student in school of microelectronics, Shandong University. He received his B.S. degree in 2017 from China University of Petroleum. His current research is mainly focused on field-effect transistor and logic circuit based on two-dimensional materials, biological and piezoelectric sensors.

Qilu Liu is a master student in Prof. Hong Liu's group in State Key Laboratory of Crystal Materials, Shandong University, China since September 2018. His research interests are structure and properties of lithium niobate crystals, ferroelectric and piezoelectric materials.

Prof. Dr. Xiaotao Hao is now a professor working at School of Physics in Shandong University, China. He is also a key member of the State Key Laboratory of Crystal Materials and a specialist of China “National Young Thousand Talent Program”. Prior to returning China in 2012, he had worked at several research institutions in Australia, Japan and Singapore. His current research interests are physics of organic optoelectronic materials and devices, time resolved fluorescence spectroscopy/microscopy, etc.

Prof. Dr. Lin Han received her B.S. degree in physics and microelectronics from Shandong University, China, in 2003, M.S. degree in microelectronics from Tsinghua University in 2006, and Ph.D. degree in electrical engineering from Princeton University, USA, in 2011. She was an Associate Postdoctoral/Research Scientist in Biomedical Engineering at Yale University between 2011 and 2015. She has been a professor at Shandong University since 2016. Her research focuses on 2D materials and devices, biosensors, microfluidic chip for bioengineering, flexible electronics, etc.

Prof. Dr. Jian-Jun Wang is a professor in State Key Laboratory of Crystal Materials, Shandong University. He received his PhD degree in 2012 from Institute of Chemistry, Chinese Academy of Science (ICCAS). His research activities are focused on challenges related to inorganic nanostructure in energy and environment field, including material fabrication, physical properties and applications, aiming to develop functional materials for photodetectors, solar cells, water splitting, sensing etc.

Prof. Dr. Caofeng Pan received his B.S. degree (2005) and his Ph.D. (2010) in Materials Science and Engineering from Tsinghua University, China. He is currently a professor and a group leader at Beijing Institute of Nanoenergy and Nanosystems, Chinese Academy of Sciences since 2013. His main research interests focus on the fields of piezotronics/piezo-phototronics for fabricating new electronic and optoelectronic devices, nano-power source (such as nanofuel cell, nano biofuel cell and nanogenerator), hybrid nanogenerators, and self-powered nanosystems.

Prof. Dr. Hong Liu is a professor in State Key Laboratory of Crystal Materials, Shandong University. He received his Ph.D. degree in 2001 from Shandong University (China). His current research is mainly focused on chemical processing of nanomaterials for energy related applications including photocatalysis, tissue engineering, especially the interaction between stem cell and nanostructure of biomaterials, as well as the nonlinear optical crystals.

Prof. Dr. Yuanhua Sang obtained his B.S. degree at Shandong University in China in 2007 and received his Ph.D degree at Shandong University in July 2012. Now, he works as an associate professor in State Key Laboratory of Crystal Materials, Shandong University, China. His research interests are structure and property investigation of inorganic crystal materials with neutron and x-ray diffraction, functional materials, and nano-materials for solar light conversion, especially for the photocatalysis and photothermal application.